Characterisation of thermionic emission current with a laser-heated system (EP)

Hugo Dominguez-Andrade (iD), Alex Croot, Gary Wan (iD), James A. Smith, and Neil A. Fox

COLLECTIONS

EP   This paper was selected as an Editor's Pick

View Online   Export Citation   CrossMark

AFM & NSOM   Nanopositioning Systems   Micropositioning   Single Molecule Microscopes

Characterisation of thermionic emission current with a laser-heated system (EP)

Hugo Dominguez-Andrade,[1,a] (iD) Alex Croot,[1] Gary Wan,[1] (iD) James A. Smith,[2] and Neil A. Fox[1,2]

AFFILIATIONS

[1] School of Physics, H.H. Wills Physics Laboratory, University of Bristol, Bristol, United Kingdom
[2] School of Chemistry, University of Bristol, Cantocks Close, Bristol BS8 1TS, United Kingdom

[a] Author to whom correspondence should be addressed: hd1313@bristol.ac.uk

ABSTRACT

Thermionic emitting materials are relevant for several technological applications like electron guns, X-ray sources, or thermionic energy converters. As new materials and surface functionalisations that enable thermionic emission are developed, it is essential to be able to test them in a repeatable and reliable manner. Here, we present a CO_2 laser-heated system for thermionic tests that can be used to test the thermionic emission current of different materials regardless of the optical properties or form factor. Our system can reach sample temperatures of $T \approx 1000$ °C and can follow pre-programmed heating profiles. Additionally, a double thermo-electrical decoupling provides a very low electrical noise environment while keeping the sample heat loss to a minimum. Experimental data on sample temperature and thermionic current from a hydrogen terminated single crystal diamond are presented and discussed.

Published under license by AIP Publishing. https://doi.org/10.1063/1.5088150

I. INTRODUCTION

Thermionic emission occurs when thermally excited electrons have enough energy to overcome the surface potential barrier of their host material known as work function.[1] Since the discovery of thermionic emission in the beginning of the 20th century, it has been used in numerous technologically relevant applications, such as vacuum diodes for current rectification,[2] X-ray sources,[3] electron sources,[4] and thermionic energy converters.[5,6] The Richardson-Dushman model[7] is commonly accepted as the theoretical basis for the description of the thermionic emission current and is widely used in the emission data analysis

$$J(T) = AT^2 e^{-\frac{\phi}{kT}}, \qquad (1)$$

where J is the thermionic current in A cm^{-2}, T is the temperature in kelvin, ϕ is the work function, k is the Boltzmann constant, and $A = 120$ A cm^{-2} K^{-2} is the Richardson constant.[8]

Typical materials used for thermionic emission include thoriated tungsten,[9] caesium oxide terminated molybdenum,[10] and LaB$_6$.[11] While more recently, materials such as carbon nanotubes,[12,13] diamond,[14] and GaN[6] have sparked a renewed interest in the field. In the case of diamond and GaN, they rely on specific surface terminations like hydrogen and caesium, respectively, in

order to lower the work function of the surface, inducing a negative electron affinity[15,16] that makes thermionic emission possible.

In order to test the thermionic emission on these materials, several methods can be used to heat the emitter material, including resistive heating, direct current heating with the material shaped like a filament, and electron heating. However, not all materials can be shaped like a filament and direct current heating may not be possible if the room temperature resistivity of the material is too high, e.g., nitrogen doped diamond.[17] For this reason, resistive heating is the typical method of choice and uses a resistive element, placed in the vicinity of the sample, which is heated by passing a current through it and transmits the heat to the sample via either conduction or radiation.[18] But this approach causes heating of the sample and its surroundings (sample stage), translating into significant thermal inertia of the assembly, which can hinder the temperature control of the sample. This is especially relevant as various materials of interest to thermionic applications have functionalised surfaces that are not thermally stable, making temperature measurement—and control—paramount in their effective and reproducible examination.[19,20] Additionally, the presence of electrical heating elements near the emitter and collector can cause the appearance of spurious currents that add noise to the thermionic current measurements.

Here, we present a high-vacuum laser-heated system for the testing of thermionic emitting materials. Our laser-based system solves the temperature control problems due to thermal inertia in resistive heaters and removes a possible source of leakage currents from the heating element that could cause measurement errors. Hence, the system enables a more precise and responsive temperature control of the samples. The utilisation of e-beam heaters for sample heating requires either the use of high voltage positive bias on the sample or electromagnetic focusing lenses to direct the electrons to the sample. Both approaches require a carefully designed electrical decoupling to avoid any electrical arcing, which would most surely mean a bigger chamber and a bulkier and more complex assembly inside it. So using a laser as a heat source would mean a drastically less complex and prone to failure system than an e-beam, which is easier to implement in a research environment. Our laser-heated system can be used to apply a variety of temperature profiles to the sample under test and keep an accurate control of the sample temperature, which can be tested to temperatures up to $T \approx 1000$ °C. The system can accept samples of different materials regardless of their optical properties or form factor like thin films or optically transparent conductors. Additionally, samples of different shapes and sizes can be tested in the system, ranging in diameter from ≈ 4 to 15 mm, as well as using electron collectors of different sizes and materials. A sample of hydrogen terminated nitrogen-doped, single crystal diamond was tested for thermionic emission and used as a demonstrator of the system's capabilities.

Previous studies report similar efforts toward a non-resistive heating mechanism for thermionic emission tests by using an infrared lamp or a pulsed laser. However, in the case of the infrared lamp,[21] whose emitted light is not directional, it does not solve the problem of thermal inertia as it also heats up the sample stage, and this hinders temperature control. On the other hand, in the case of previous laser systems,[22] the laser power was insufficient to heat samples larger than a few millimetres and the problem of heating materials with different optical properties was not addressed. The issues mentioned above are all addressed in the current study. Other laser-heated systems were developed, but they were focused on the testing of electron guns[23] or spectroscopy[24] systems and therefore had a different purpose of the system being described here.

II. INSTRUMENT

The instrument has three main components: a heating system, an emitter-collector assembly, and a current measurement circuit. The heating system uses a CO_2 laser to heat the sample, while the temperature is monitored by infrared pyrometry and

thermocouples. The sample sits on the emitter-collector assembly that is housed inside a high vacuum chamber pumped by a turbo molecular pump (Edwards EXT 75DX CF63, Edwards Ltd.) and a scroll pump (Scrollvac SC 30D, Leybold Ltd.). This allows for a system base pressure of $\approx 1 \times 10^{-6}$ mTorr. The sample temperature control, laser, and logging of all data are performed by a Labview virtual instrument. This software integrates all the components of the system and uses a Proportional-Integral-Derivative (PID) closed loop controller to regulate the emitter temperature [see Fig. 1(a)].

A. Emitter–collector assembly

The emitter-collector assembly is shown in Fig. 2. The emitter (or sample) rests on a quartz plate that acts as a layer providing thermo-electrical decoupling, avoiding both heat loss and electrical interference with the rest of the structure. The sample is locked in place with molybdenum clamps, which are attached to the quartz plate and used as electrical contacts. An area of the quartz plate beneath the sample has been machined to provide an aperture with a diameter of ≈ 8 mm for the laser to reach the back of the sample. The quartz plate is attached onto a detachable stainless steel hollow cylinder that can be easily removed from the system to facilitate sample exchange. The cylinder sits on another machined quartz plate acting as a second layer of thermo-electrical decoupling. Previous experience with similar thermionic systems showed that spurious leakage currents were a major problem for precise and reproducible current measurements, and the double thermo-electrical decoupling implemented in this system is meant to avoid such complications. Quartz was chosen as the decoupling material owing to its electrical and thermally insulating properties ($k \approx 1.5$ W m^{-1} K^{-1}).[25] However, above 1050 °C, quartz suffers from a loss of mechanical integrity, limiting the maximum operating temperature of the system. In cases where higher sample temperatures are required, quartz can be replaced by pyrolytic boron nitride, which has a better tolerance at high temperatures. The second quartz plate sits on a stainless steel square frame attached in the four corners to four steel rods, which are in turn connected to the top flange of the vacuum chamber so that the emitter stage is suspended from this flange.

Above the sample stage sits the collector assembly that harvests electrons emitted by the sample. The collector assembly consists of a cylindrical molybdenum collector that can be easily exchanged with others of different materials and sizes. The collector is attached to a thermo-electrical decoupler (made of a machinable borosilicate ceramic known commercially as Macor®), which in turn is connected to a vacuum-compatible linear shift motor (Z825BV, Thorlabs, Inc.). This decoupler has three functions: it avoids any electrical noise caused by the motor from reaching the collector; it isolates the
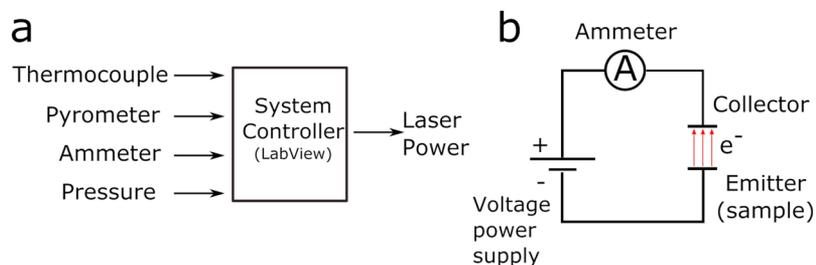
a

Thermocouple →
Pyrometer →   System Controller (LabView) → Laser Power
Ammeter →
Pressure →

b

Ammeter
(A)

Collector
e⁻
Emitter (sample)

+
−
Voltage power supply

FIG. 1. (a) Control system diagram with the input and output signal logged by the system. This controller has been implemented as a virtual instrument in Labview and includes a Proportional-Integral-Derivative (PID) feedback loop controller for the temperature control. (b) Current measurement circuit diagram of the instrument.
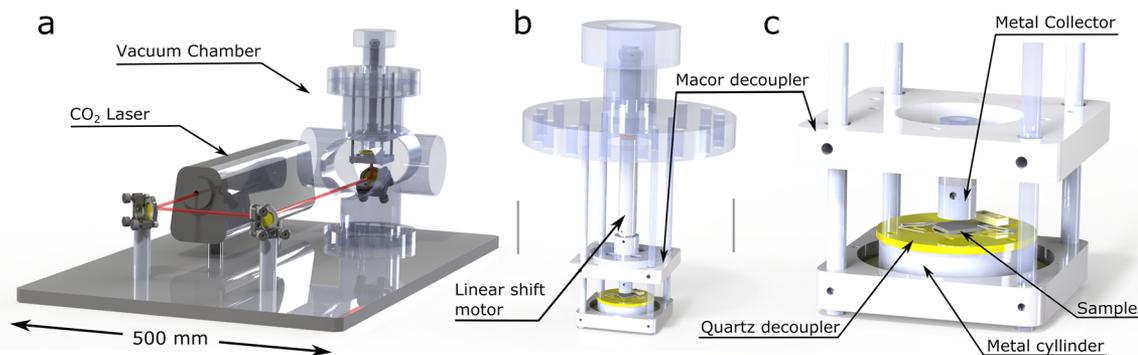
FIG. 2. Thermionic testing system diagram. (a) Whole system with the CO_2 laser source and vacuum chamber. The laser beam path is shown in red. (b) Instrument assembly from inside the vacuum chamber, showing the linear shift that holds the collector, mounted on a Macor thermo-electrical decoupler. (c) Emitter-collector assembly showing the emitter (sample) mounted on a thermo-electrically decoupling quartz plate. The quartz plate is attached to a removable stainless steel cylinder in order to facilitate sample exchange.

linear shift from the voltage bias applied to the collector; and it protects the motor from the high temperatures reached in the adjacent collector. With this configuration, the maximum temperature reached in the collector is ≈ 300 $^\circ$C while the motor temperature never goes above 60 $^\circ$C. The linear shift is used to control the gap distance between the emitter and collector prior to and during experiments. It has a theoretical spatial resolution of 40 nm, but it is limited by the backslash of the reduction box incorporated in the motor, so the actual linear resolution is ≈ 1 μm. The linear shift is mounted onto the thermo-electrical decoupling Macor square plate attached to the four stainless steel rods suspended from the top flange of the chamber.

While performing current measurements, the system operates in a close circuit fashion [see Fig. 1(b)] where the different elements are connected in series, namely, the emitter-collector diode, a DC power supply (Mastech Linear DC power supply—HY3003D, Mastech.), and an ammeter (Keithley 2750 Multimeter system, Tektronix) with an uncertainty of $U_J = \pm$(ppm reading + ppm range), where ppm = parts per million. The power supply applies a positive voltage bias to the collector in order to harvest the emitted electrons so that the thermionic current can be measured by the ammeter [see Fig. 1(b)].

B. Heating system

The emitter is heated by a continuous wave CO_2 laser (Firestar V40 series, Synrad) with a wavelength of 10.6 μm and a maximum output power of $P_L = 40$ W. The beam diameter at the exit of the laser is 2.5 mm with a divergence of <7 mrad, and it is linearly polarised and has a TEM 00 mode. The laser beam is guided toward the vacuum chamber with gold coated copper mirrors and feeds into the chamber through a ZnSe window (WG71050-G, Thorlabs, Inc.). Once inside the chamber, the beam is deflected upwards with another gold coated copper mirror so that it can reach the sample [see Fig. 1(a)]. By the time the laser reaches the sample, the beam has an approximate diameter of ≈ 6 mm and experiences an $\approx 25\%$ power reduction due to optical losses. The heating system is controlled by a Labview virtual instrument that operates a closed loop

so that the temperature is maintained at the desired level. The temperature of the sample can be set to follow predefined ramps and a number of heating-cooling cycles. The system has been shown to be able to maintain the sample temperature with a maximum deviation of 0.5 $^\circ$C with respect to the temperature setpoint.

The CO_2 laser can heat any material provided, and it possesses enough optical absorbance at the wavelength of the laser. Hence, T_{max}, the maximum attainable temperature on the sample, is a function of this absorbance. Three approaches were tried in order to achieve a high T_{max} during experiments independently of the testing material, namely, high absorbance sample materials, enhancing absorbance via amorphous carbon deposition and enhancing absorbance via plasmonic gratings.[26] In the first case, we used polycrystalline boron doped diamond, which has a high absorbance for the CO_2 laser, and could reach $T_{max} \approx 1000$ $^\circ$C for the maximum laser output power. For the second approach, amorphous carbon was deposited on the back of a single crystal diamond in a microwave plasma chemical vapour deposition (CVD) reactor, increasing the absorbance and providing a maximum temperature of $T_{max} \approx 920$ $^\circ$C. This was a significant improvement over the uncoated diamond sample where T_{max} was about 300 $^\circ$C. In the third approach, we used plasmonic gratings engraved in molybdenum foils tailored to increase the absorbance at the wavelength of the CO_2 laser. These reached a T_{max} of 1100 $^\circ$C as we reported previously.[27] Having a variety of approaches to increase the laser absorbance and consequently T_{max} facilitates the examination of a wide range of materials up to $T_{max} \approx 1000$ $^\circ$C. Hence, it is possible to test very thin films by depositing them on molybdenum or thick single or polycrystalline materials with a low absorbance by direct exposure to the laser after applying a carbon coating.

C. Temperature measurement

Thermionic emission current is extremely sensitive to the temperature of the emitter due to its quadratic dependence on the temperature as it is shown by the Richardson-Dushman equation [Eq. (1)]. Therefore, great care has to be taken in order to achieve accurate temperature readings and temperature control, as a small

change in temperature will cause a great change in the thermionic current. Both a two-colour infrared pyrometer and a thermocouple simultaneously measure the sample temperature during experiments. The thermocouple is a standard type-K thermocouple with a measurement range of −200 °C to 1350 °C, and it is firmly pressed against the sample to ensure a good contact throughout the experiment. The resolution of the thermocouple is $R_{TC} = 0.1$ K and the uncertainty $U_{TC} = \pm 7.5 \times 10^{-3} \times T$ or 2.2 K, whichever is higher.

The two-colour infrared pyrometer (Spotmeter R160, Land Instruments International Ltd.) has two detectors each sensitive to a different wavelength: detector 1: $\lambda_1 = 1.0$ μm and detector 2: $\lambda_2 = 1.5$ μm. This allows the pyrometer to measure using one of the two detectors (single mode) or both at the same time (ratio mode). The measurements in ratio mode are independent of the different emissivities ($\varepsilon_1, \varepsilon_2$) of the material for the wavelengths of the two detectors and therefore improves the accuracy of the measurements, but it is still necessary to know the ratio between the two emissivities ($r = \varepsilon_1/\varepsilon_2$). The temperature range of the pyrometer combining the two detectors is 250 °C to 1600 °C, while the ratio mode range is 550 °C–1600 °C. The resolution of the pyrometer is $R_P = 0.1$ K and the uncertainty $U_P = \pm 2.5 \times 10^{-3} \times T$ or 2 K, whichever is higher. The pyrometer is focused on the back of the sample heated by the laser through a borosilicate window (Kodial®) with a high optical transmission for the wavelengths of the pyrometer detectors.

In our experiments, the thermocouple is used to measure the temperature of the sample on the low temperature range until it is in the range of the pyrometer ($T > 280$ °C) after which the pyrometer is employed using only one detector (detector 2) with an adjusted emissivity ε_2. This emissivity was found by previously calibrating the detector 2 against the pyrometer itself working in ratio mode. This strategy extends the pyrometer temperature minimum range from 550 °C down to 280 °C, providing a smooth an accurate reading of the temperature across all the experiment temperatures.

III. RESULTS

A. Sample temperature

The temperature of a single crystal diamond was monitored while being heated on the system following a temperature ramp of 1 °C/s. The temperature of the sample measured by the thermocouple, when compared to that of the pyrometer, presents a temperature deviation $\Delta T = T_{pyro} - T_{Th}$ that increases with temperature (see Fig. 3). In the case of diamond, its high phonon frequencies result in the appearance of a thermal contact resistance when placed in contact with other lower phonon frequency materials.[28] This causes the thermocouple to measure a temperature lower than that of the diamond sample but does not affect the pyrometer measurements. Due to this phenomenon, the temperature deviation is $\Delta T \approx 20$ °C at 300 °C, becoming more relevant at higher temperatures, where ΔT reaches a value of ≈ 50 °C. Such variation in ΔT indicates that in the examined temperature regime, the pyrometer is a more reliable source for temperature measurements. Other materials might exhibit the same temperature deviation described above but as diamond is the material with the highest phonon frequency, it is expected that the temperature deviation on other materials will be less significant.
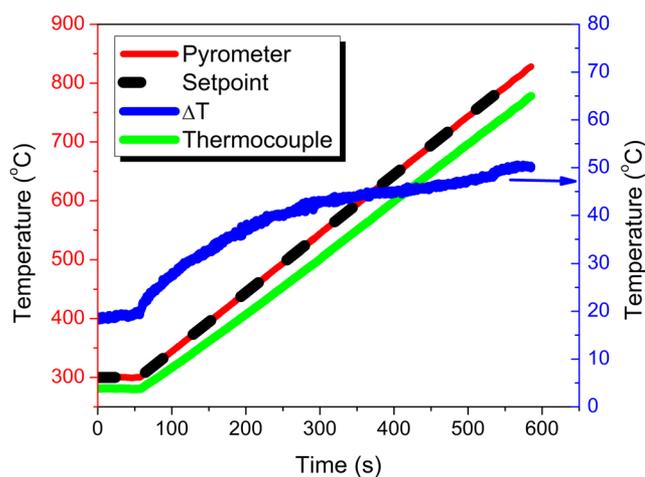

FIG. 3. Laser heated single crystal diamond temperature over time. Red line: temperature measured by the two-colour pyrometer. Black dashed line: temperature setpoint specified in the control system. Blue line: temperature difference between the pyrometer and the thermocouple. Green line: temperature measured by the thermocouple. The resolution of the pyrometer is $R_P = 0.1$ K and the uncertainty $U_P = \pm 2.5 \times 10^{-3} \times T$ or 2 K, whichever is higher. The resolution of the thermocouple is $R_{TC} = 0.1$ K and the uncertainty $U_{TC} = \pm 7.5 \times 10^{-3} \times T$ or 2.2 K, whichever is higher.

B. Thermionic emission measurements

The thermionic emission from a sample of hydrogen-terminated, nitrogen-doped, single crystal diamond was tested in the system. The diamond was hydrogen-terminated by exposing the surface to a hydrogen plasma generated on a microwave CVD reactor with a H_2 flow of 300 SCCM, $P = 1.5$ kW, pressure = 100 Torr, and a substrate temperature of $T_{subs} \approx 470$ °C for $t = 2$ min to ensure full surface coverage. The single crystal diamond had a square shape with a size of roughly 9.8 × 9.8 mm and a thickness of 0.4 mm. The collector used was made of molybdenum and had a cylindrical shape with a diameter of 10 mm with the sample-facing side of the collector polished to a mirror finish. A positive voltage bias of $V_{bias} = 25$ V was applied to the collector which was placed 200 μm away from the sample. This created an electric field of E = 1.25 × 10^5 V/m between the sample and collector. The sample temperature followed a triangular profile with a start temperature of $T_{start} = 300$ °C and ramping up to $T_{max} = 900$ °C at a rate of $\beta = 1$ °C/s. Immediately after that, the temperature was ramped down to T_{start} at the same rate. This thermal cycle was repeated several times as it is shown by the temperature profile of the experiment in Fig. 4(a).

The thermionic current emitted by the sample during the heating cycles is shown in Fig. 4(b). In the first heating cycle, the maximum current is $J_1 \approx 1 \times 10^{-4}$ mA cm^{-2}. From close examination of the data, it seems to follow an exponential trend as the temperature increases before the current maximum, which is compatible with the Richardson-Dushman model [Eq. (1)]. After the current maximum, the thermionic current decreases indicating a hydrogen thermal desorption from the surface.[29,30] Consequently, each subsequent heating cycle shows a similar qualitative behavior but with a decrease of the maximum thermionic current compared to its
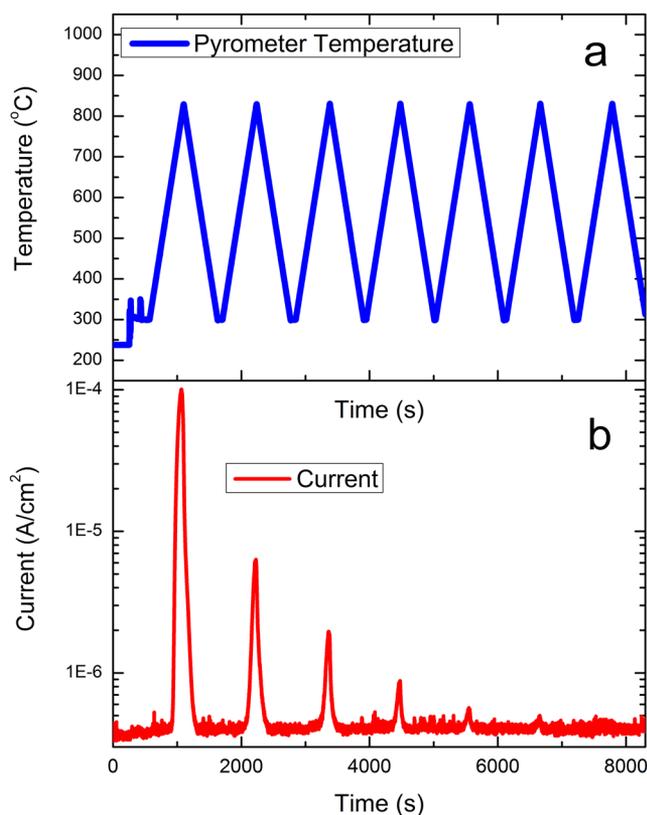
FIG. 4. Raw temperature (a) and thermionic current (b) data plots from a hydrogen terminated single crystal diamond produced by continuous heating cycles. The resolution of the pyrometer is $R_P = 0.1$ K and the uncertainty $U_P = 2.5 \times 10^{-3} \times T$ or 2 K, whichever is higher. The uncertainty of the measurements for this current range is always below $U_J = \pm 6.9 \times 10^{-7}$ A.

FIG. 5. Maximum thermionic emission currents for each heating cycle represented in Fig. 4(b). This highlights the change in emission current as the surface conditions change. The uncertainty of the measurements for this current range is always below $U_J = \pm 6.9 \times 10^{-7}$ A.

previous counterpart. The decrease in the maximum thermionic current for each of the heating cycles is plotted in Fig. 5.

Traditionally, the thermionic emission data are analyzed by fitting the Richardson-Dushman model [Eq. (1)] to the experimental data assuming a stable surface and a constant work function at all temperatures. However, in the case of unstable surfaces like hydrogen terminated diamond, these assumptions only hold true in the lower temperature region. Fitting Eq. (1) to the experimental data of the 1st heating cycle shows a work function $\phi \approx 1.5$ eV $\pm$ 0.1 eV, with a Richardson constant value of $A = 79$ A cm^{-2} K^{-2}. But, subsequent heating cycles seem to modify the surface which in turn modifies the work function. Therefore, the use of the Richardson-Dushman model on this type of unstable surfaces should be made with caution. A detailed discussion on this particular issue can be found elsewhere.[31]

Due to the changing character of the functionalised surface and its critical influence over the thermionic current, it is especially important to maintain accurate control of the sample temperature throughout a heating cycle. Otherwise, the lack of sufficient control would preclude experimental reproducibility as different conditions would cause a di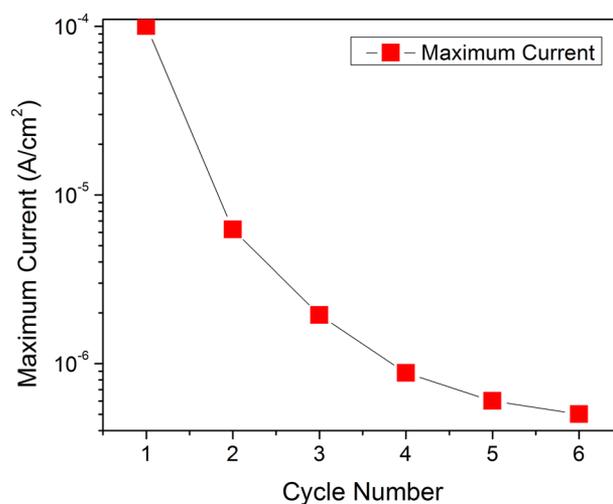fferent evolution of the surface during the heating cycles and consequently significant changes in the thermionic current experimental data.

IV. CONCLUSIONS

The main advantages of the experimental system presented here are the fine control of the sample temperature, the modularity of the system, and the possibility to test a wide variety of materials. These capabilities enable the system for a detailed study of the effects of thermally unstable surfaces on the thermionic emission characteristics of emitting materials. Additionally, traditional thermally stable surfaces can also be successfully tested.

As an example of the use of the system, we have studied hydrogen terminated diamond, which is a thermionic emitter but has a thermally unstable surface. Thermionic emission data were successfully collected from this sample on a series of consecutive heating cycles confirming the changing behavior of the diamond emitting surface. Moreover, the work function of the hydrogenated surface was extracted from the first cycle showing a value of $\phi \approx 1.5$ eV $\pm$ 0.1 eV.

The results presented here are just an example of the multiple experiments that can be made using the system as there are a variety of parameters that can be explored on future research. As an example, it is possible to decrease the gap between the collector and emitter and study its effects on the collected current with or without bias. In the latter case, changing the material of the collector can be used to study the collection efficiency of different materials in order to make progress toward a thermionic energy converter.[32]

REFERENCES

[1] N. D. Lang and W. Kohn, Phys. Rev. B **3**, 1215 (1971).

[2] M. Guarnieri, IEEE Ind. Electron. Mag. **6**, 41 (2012).

[3] W. D. Coolidge, Phys. Rev. **2**, 409 (1913).

[4] I. D. Baikie, U. Peterman, B. Lägel, and K. Dirscherl, J. Vac. Sci. Technol., A **19**, 1460 (2001).

[5] G. N. Hatsopoulos and E. P. Gyftopoulos, *Thermionic Energy Conversion*, Processes and Devices (The MIT Press, 1973), Vol. I.

[6] J. W. Schwede, I. Bargatin, D. C. Riley, B. E. Hardin, S. J. Rosenthal, Y. Sun, F. Schmitt, P. Pianetta, R. T. Howe, Z.-X. Shen, and N. A. Melosh, Nat. Mater. **9**, 762 (2010).

[7] O. W. Richardson, *Nobel Lecture* (Nobel Media, 1929).

[8] C. R. Crowell, Solid-State Electron. **8**, 395 (1965).

[9] A. King, Phys. Rev. **53**, 570 (1938).

[10] K. P. Loh, X. N. Xie, S. W. Yang, J. S. Pan, and P. Wu, Diamond Relat. Mater. **11**, 1379 (2002).

[11] A. V. Bulyga and V. K. Solonovich, Surf. Sci. **223**, 578 (1989).

[12] P. Liu, Q. Sun, F. Zhu, K. Liu, K. Jiang, L. Liu, Q. Li, and S. Fan, Nano Lett. **8**, 647 (2008).

[13] C. V. Dharmadhikari, P. S. Alegaonkar, S. K. Kolekar, S. P. Patole, and J. B. Yoo, Appl. Surf. Sci. **257**, 10306 (2011).

[14] F. A. M. Koeck, R. J. Nemanich, Y. Balasubramaniam, K. Haenen, and J. Sharp, Diamond Relat. Mater. **20**, 1229 (2011).

[15] D. Takeuchi, S.-G. Ri, H. Kato, C. E. Nebel, and S. Yamasaki, Phys. Status Solidi A **202**, 2098 (2005).

[16] H. Ibach, *Physics of Surfaces and Interfaces* (Springer Berlin Heidelberg, 2006).

[17] S. Koizumi, C. Nebel, and M. Nesladek, *Physics and Applications of CVD Diamond* (Wiley-VCH Verlag GmbH & Co. KGaA, Weinheim, Germany, 2008).

[18] F. A. M. Koeck and R. J. Nemanich, Diamond Relat. Mater. **15**, 217 (2006).

[19] W. F. Paxton, M. M. Brooks, M. Howell, N. Tolk, W. P. Kang, and J. L. Davidson, J. Appl. Phys. **115**, 234904 (2014).

[20] K. P. Loh, J. S. Foord, R. G. Egdell, and R. Jackman, Diamond Relat. Mater. **6**, 874 (1997).

[21] M. Suzuki, T. Ono, N. Sakuma, and T. Sakai, Diamond Relat. Mater. **18**, 1274 (2009).

[22] Z. Li, B. Bai, C. Li, and Q. Dai, Carbon **96**, 641 (2016).

[23] P. K. Roy, A. Moon, K. Mima, S. Nakai, M. Fujita, K. Imasaki, C. Yamanaka, E. Yasuda, T. Watanabe, N. Ohigashi, Y. Okuda, and Y. Tsunawaki, Rev. Sci. Instrum. **67**, 4098 (1996).

[24] T. A. Yager and W. D. Kingery, Rev. Sci. Instrum. **51**, 464 (1980).

[25] I. M. Abdulagatov, S. N. Emirov, T. A. Tsomaeva, K. A. Gairbekov, S. Y. Askerov, and N. A. Magomedova, J. Phys. Chem. Solids **61**, 779 (2000).

[26] U. Guler, A. Boltasseva, and V. M. Shalaev, Science **344**, 263 (2014).

[27] S. Nunez-Sanchez, H. D. Andrade, J. Harwood, I. Bickerton, N. A. Fox, and M. J. Cryan, Micro Nano Lett. **13**, 1325 (2018).

[28] J. Anaya, H. Sun, J. Pomeroy, and M. Kuball, in *2016 15th IEEE Intersociety Conference on Thermal and Thermomechanical Phenomena in Electronic Systems (ITherm)* (IEEE, 2016), pp. 1558–1565.

[29] S. Elfimchev, S. Michaelson, R. Akhvlediani, M. Chandran, H. Kaslasi, and A. Hoffman, Phys. Status Solidi A **211**, 2238 (2014).

[30] W. F. Paxton, M. Howell, W. P. Kang, and J. L. Davidson, J. Vac. Sci. Technol., B: Nanotechnol. Microelectron.: Mater., Process., Meas., Phenom. **30**, 021202 (2012).

[31] H. Dominguez-Andrade, J. Anaya, A. Croot, M. Cattelan, D. J. Twitchen, M. Kuball, and N. A. Fox, "Correlating thermionic emission with specific surface reconstructions in ⟨100⟩ hydrogenated single crystal diamond" (unpublished).

[32] E. van Kemenade and W. Veltkamp, in *Intersociety Energy Conversion Engineering Conference* (American Institute of Aeronautics and Astronautics, Reston, Virigina, 1994).